Properties of strongly interacting QCD matter

Elena Bratkovskaya
(GSI, Darmstadt & Uni. Frankfurt)

10th International Symposium on Non-equilibrium Dynamics (NeD-2024)
25 - 29 November, 2024
Krabi, Thailand

Properties of strongly interacting QCD matter

The phase diagram of QCD → thermal properties of QCD in the (T, μ_B) plane → probed by heavy-ion collisions (non-equilibrium dynamics)

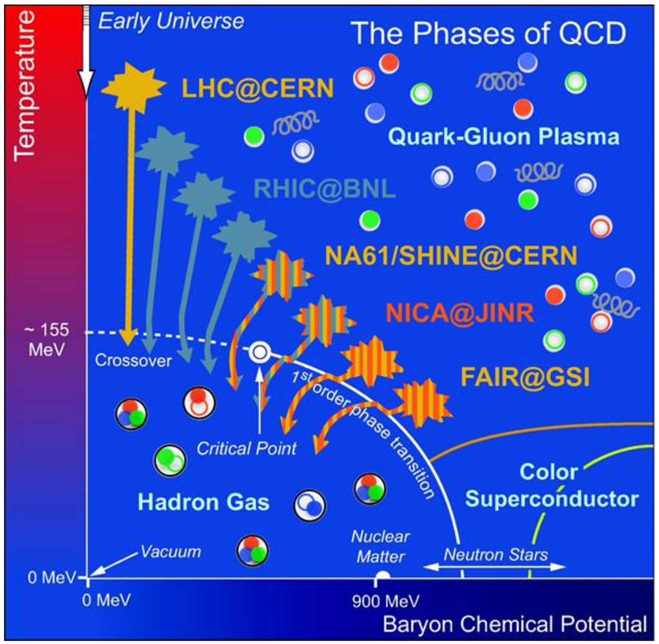

The goal:

to describe the dynamics of partonic and hadronic degrees-of-fredom and their interactions on a microscopic basis

Realization:

a dynamical non-equilibrium transport approach

- **applicable for strongly interacting systems,**
- **which includes a phase transition from hadronic matter to QGP**

The tool:

PHSD/PHQMD approach

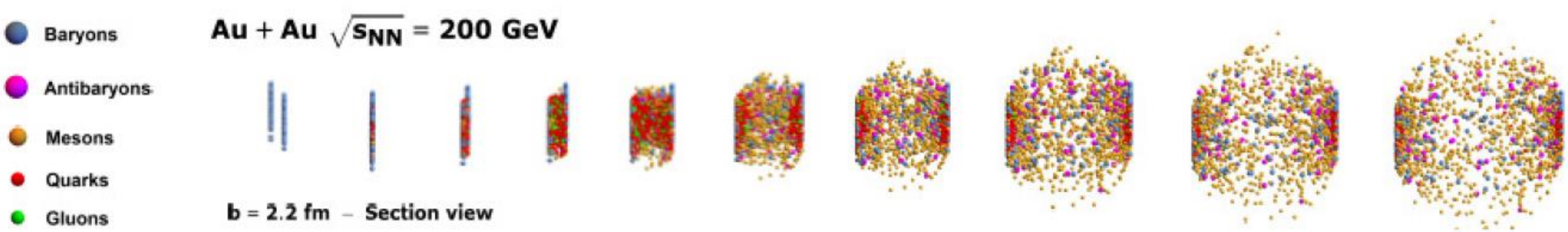

Degrees-of-freedom of QGP

lQCD: QGP EoS at finite μ_B

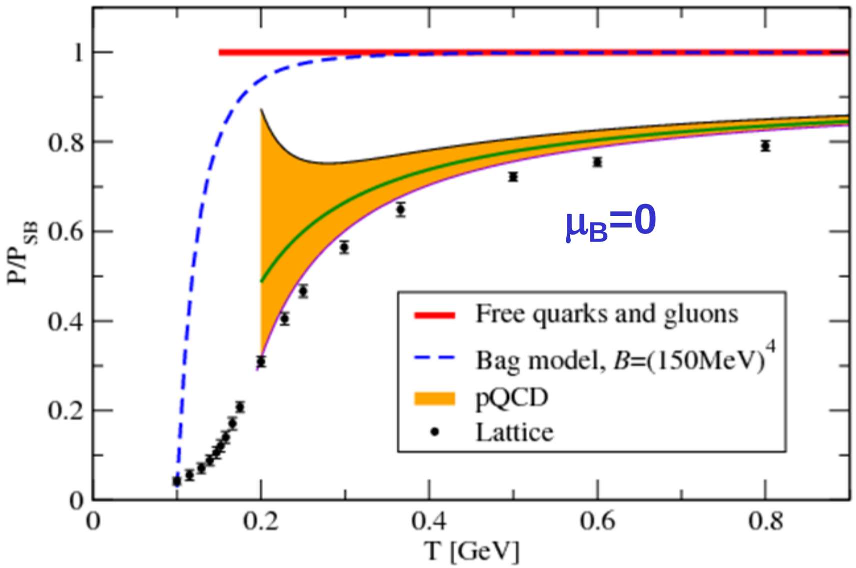

Non-perturbative QCD ← pQCD

pQCD: (Yang-Mills) shear viscosity η

J. Ghiglieri, G.D. Moore, D. Teaney, JHEP 1803 (2018) 179

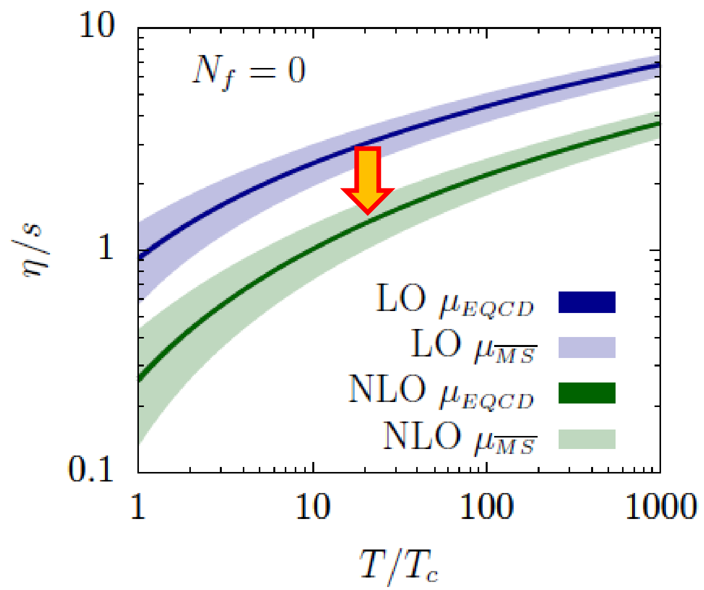

pQCD:

- ❑ **weakly interacting system**
- ❑ **massless quarks and gluons**

Thermal (non-perturbative) QCD:

- ❑ **strongly interacting system**
- ❑ **massive quarks and gluons**

➔ Quasiparticles = effective degrees-of-freedom

Thermal QCD →

DQPM (T, μ_q)

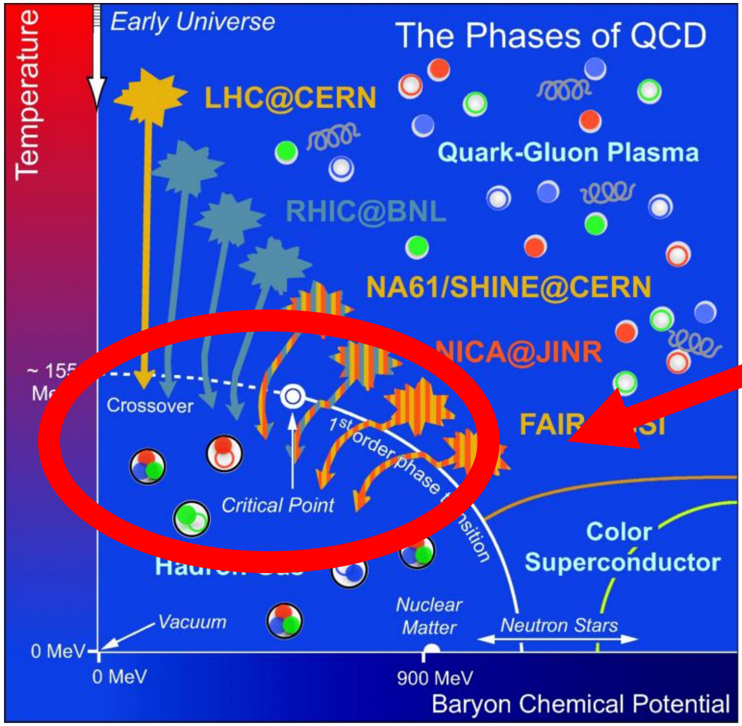

finite T, μ_q

Dynamical QuasiParticle Model (DQPM)

DQPM – effective model for the description of non-perturbative (strongly interacting) QCD based on lQCD EoS

Degrees-of-freedom: strongly interacting dynamical quasiparticles - quarks and gluons

Theoretical basis :

- ‚resummed' single-particle Green's functions → quark (gluon) propagator (2PI) :

gluon propagator: $\Delta^{-1} = P^2 - \Pi$	&	quark propagator $S_q^{-1} = P^2 - \Sigma_q$
gluon self-energy: $\Pi = M_g^2 - i2\gamma_g\omega$	&	quark self-energy: $\Sigma_q = M_q^2 - i2\gamma_q\omega$

Properties of the quasiparticles are specified by scalar complex self-energies:

$Re\Sigma_q$: thermal masses (M_g, M_q); $Im\Sigma_q$: interaction widths (γ_g, γ_q)

→ spectral functions $\rho_q = -2ImS_q$ → Lorentzian form:

$$\rho_j(\omega, \mathbf{p}) = \frac{\gamma_j}{\tilde{E}_j}\left(\frac{1}{(\omega - \tilde{E}_j)^2 + \gamma_j^2} - \frac{1}{(\omega + \tilde{E}_j)^2 + \gamma_j^2}\right)$$

$$\equiv \frac{4\omega\gamma_j}{\left(\omega^2 - \mathbf{p}^2 - M_j^2\right)^2 + 4\gamma_j^2\omega^2} \qquad \tilde{E}_j^2(\mathbf{p}) = \mathbf{p}^2 + M_j^2 - \gamma_j^2$$

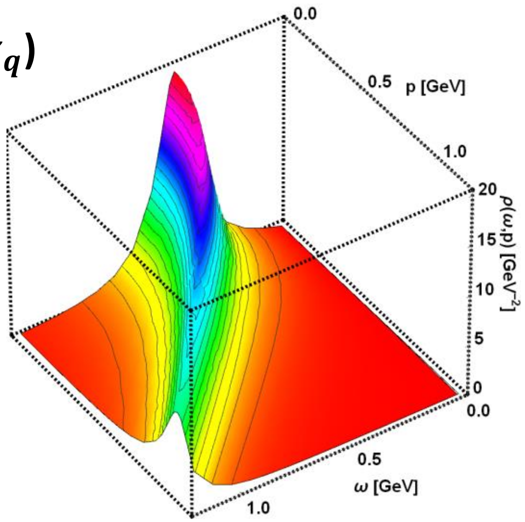

A. Peshier, W. Cassing, PRL 94 (2005) 172301; W. Cassing, NPA 791 (2007) 365: NPA 793 (2007), H. Berrehrah et al, Int.J.Mod.Phys. E25 (2016) 1642003; P. Moreau et al., PRC100 (2019) 014911; O. Soloveva et al., PRC101 (2020) 045203

DQPM: parton properties

Realization concept:

- ❑ introduce an ansatz (HTL; with few parameters) for the (T, μ_B) dependence of masses/widths
- ❑ evaluate the QGP thermodynamics in equilibrium using the Kadanoff-Baym theory
- ❑ fix DQPM parameters by comparison of the DQPM entropy density to lQCD at μ_B=0

- **Masses** and **widths** of quasiparticles depend on T and μ_B

$$m_g^2(T,\mu_B) = C_g \frac{g^2(T,\mu_B)}{6} T^2 \left(1 + \frac{N_f}{2N_c} + \frac{1}{2}\frac{\sum_q \mu_q^2}{T^2\pi^2}\right)$$

$$m_{q(\bar{q})}^2(T,\mu_B) = C_q \frac{g^2(T,\mu_B)}{4} T^2 \left(1 + \frac{\mu_q^2}{T^2\pi^2}\right)$$

$$\gamma_j(T,\mu_B) = \frac{1}{3} C_j \frac{g^2(T,\mu_B) T}{8\pi} \ln\left(\frac{2c_m}{g^2(T,\mu_B)} + 1\right)$$

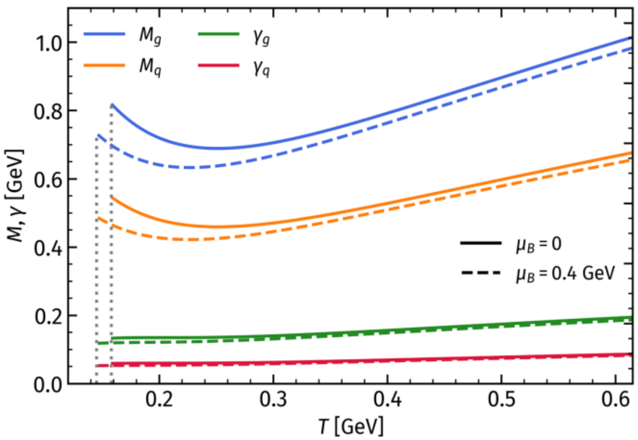

- **Strong coupling** (g) is defined from **lQCD entropy density** at μ_B=0, using $\frac{\partial}{\partial T}\left(\frac{s_{DQPM}}{T^3}\right) = 0$

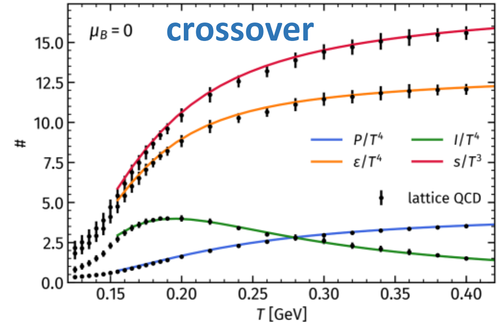

$$g^2(s/s_{SB}) = d((s/s_{SB})^e - 1)^f$$

$$s_{SB}^{QCD} = 19/9\ \pi^2 T^3$$

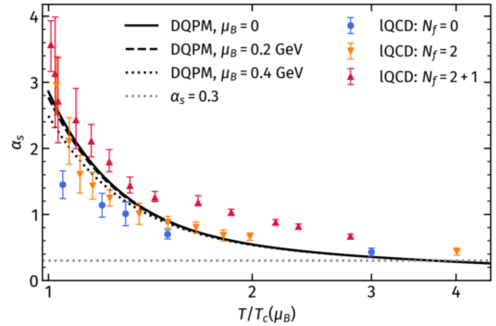

$$\alpha_s = g^2(T,\mu_B)/(4\pi)$$

➔ DQPM allows to explore QCD in the **non-perturbative regime** of the (T, μ_B) phase diagram

Partonic interactions: matrix elements

DQPM partonic cross sections → leading order diagrams

- **Propagators for massive bosons and fermions:**

$$= -i\delta_{ab} \frac{g^{\mu\nu} - q^\mu q^\nu / M_g^2}{q^2 - M_g^2 + 2i\gamma_g q_0}$$

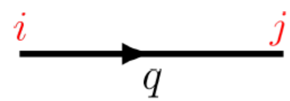

$$= i\delta_{ij} \frac{\not{q} + M_q}{q^2 - M_q^2 + 2i\gamma_q q_0}$$

- **(Quasi-) elastic channels:**

qq' → qq' scattering

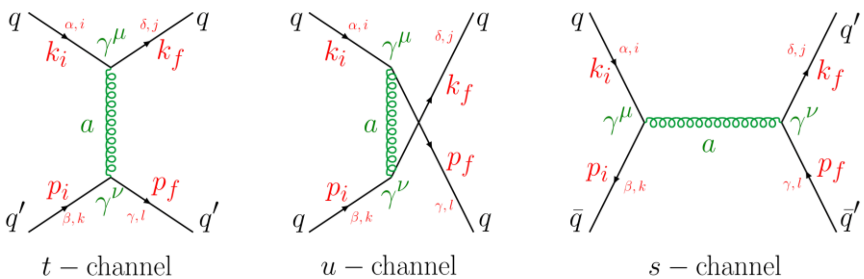

gq → gq scattering

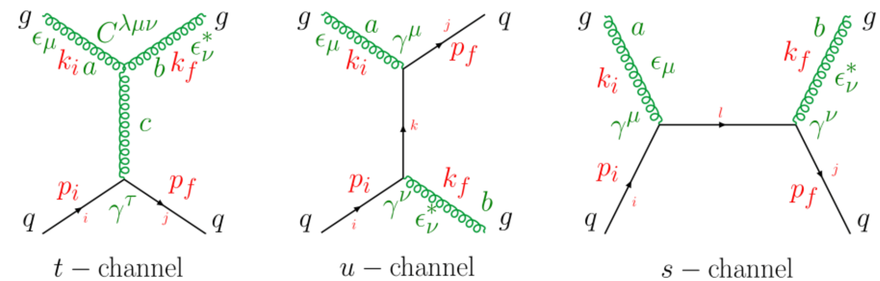

gg→ gg scattering

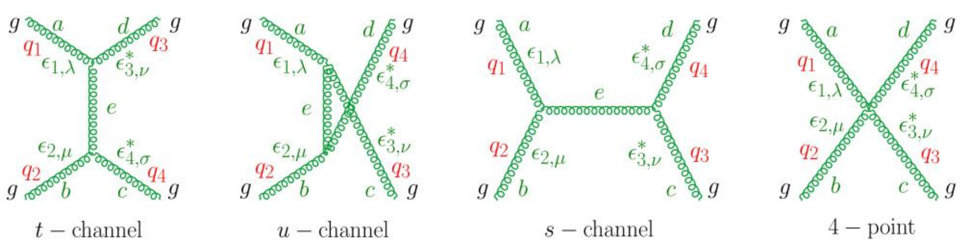

- **Inelastic channels:**

$$\mathrm{q} + \bar{\mathrm{q}} \rightarrow \mathrm{g}$$

$$\mathrm{g} \rightarrow \mathrm{q} + \bar{\mathrm{q}}$$

H. Berrehrah et al, PRC 93 (2016) 044914, Int.J.Mod.Phys. E25 (2016) 1642003, → **P. Moreau et al., PRC100 (2019) 014911**

Differential cross sections

- **On-shell:**

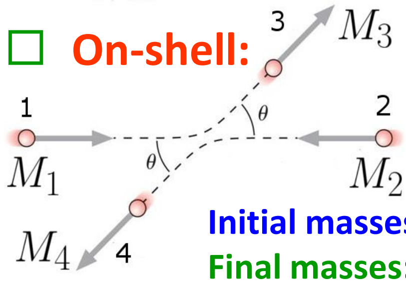

Initial masses: pole masses
Final masses: pole masses

- **Off-shell:**

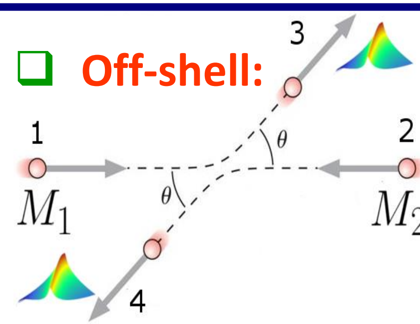

Initial masses: pole masses
Final masses: integration over spectral functions

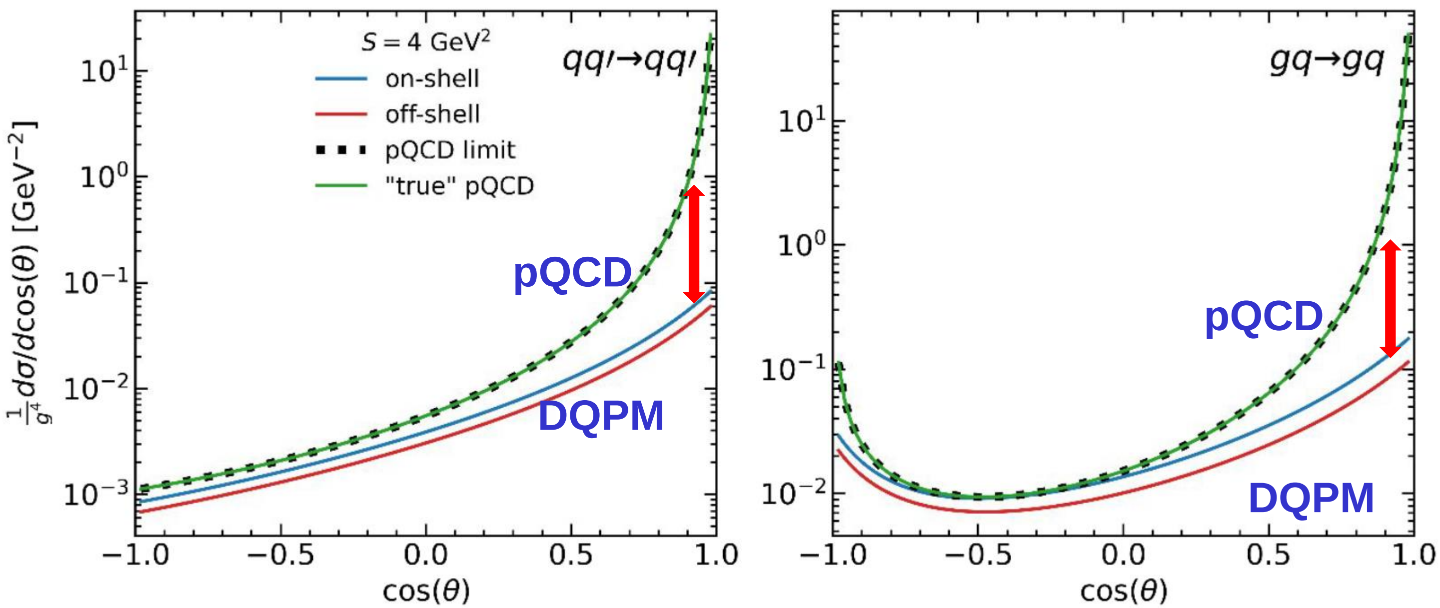

Plot by Ilia Grishmanovskii

- **DQPM: M→0, γ→0 ➔ reproduces pQCD limits**
- **Differences between DQPM and pQCD : less forward peaked angular distribution leads to more efficient momentum transfer**

P. Moreau et al., PRC100 (2019) 014911

Total elastic cross sections

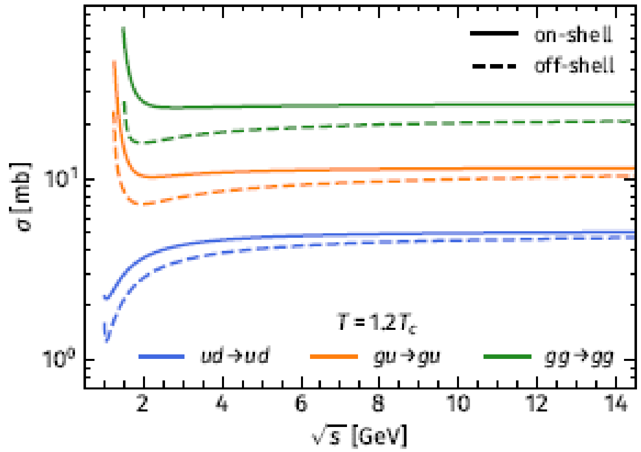

- off-shell effects are stronger at low $s^{1/2}$

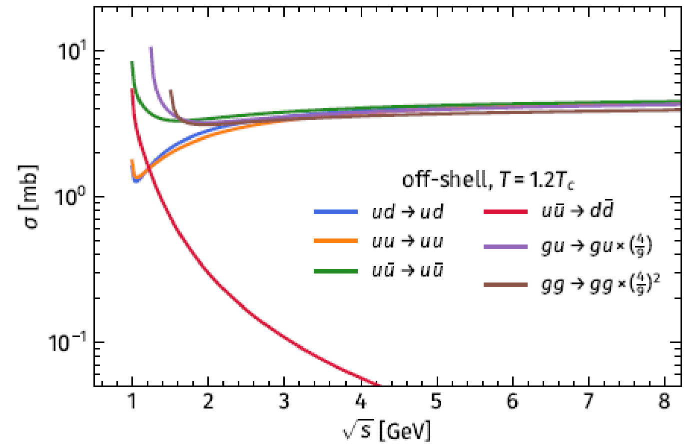

- strong channel dependence at low $s^{1/2}$

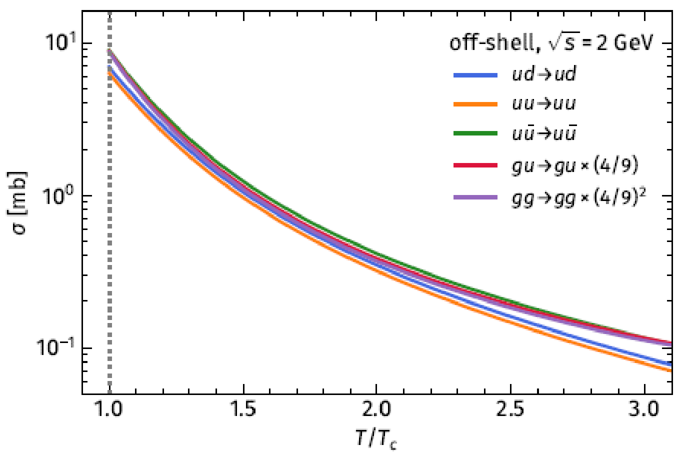

- strong *T* dependence
- ~ scaling with color ratio

$$|\overline{\mathcal{M}}_{gg}|^2 \approx \frac{C_g}{C_q}|\overline{\mathcal{M}}_{gq}|^2 \approx \left(\frac{C_g}{C_q}\right)^2 |\overline{\mathcal{M}}_{qq}|^2$$

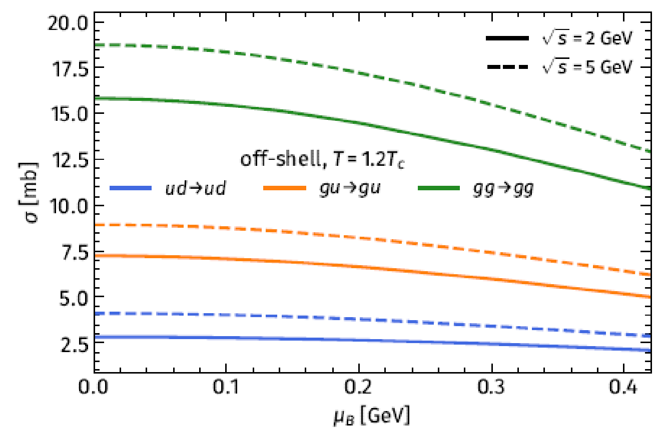

- weak μ_B dependence

I. Grishmanovskii et al., PRC 110, 014908 (2024), plots from PhD Thesis

DQPM: Mean-field potential for quasiparticles

Space-like part of energy-momentum tensor $T_{\mu\nu}$ defines the potential energy density:

$$V_p(T,\mu_q) = T^{00}_{g-}(T,\mu_q) + T^{00}_{q-}(T,\mu_q) + T^{00}_{\bar{q}-}(T,\mu_q)$$

space-like gluons + space-like quarks+antiquarks

$$\tilde{\mathrm{Tr}}^{\pm}_{g} \cdots = d_g \int \frac{d\omega}{2\pi} \frac{d^3p}{(2\pi)^3} 2\omega\, \rho_g(\omega)\, \Theta(\omega)\, n_B(\omega/T)\; \Theta(\pm P^2) \cdots$$

$$\tilde{\mathrm{Tr}}^{\pm}_{q} \cdots = d_q \int \frac{d\omega}{2\pi} \frac{d^3p}{(2\pi)^3} 2\omega\, \rho_q(\omega)\, \Theta(\omega)\, n_F((\omega-\mu_q)/T)\; \Theta(\pm P^2) \cdots$$

$$\tilde{\mathrm{Tr}}^{\pm}_{\bar{q}} \cdots = d_{\bar{q}} \int \frac{d\omega}{2\pi} \frac{d^3p}{(2\pi)^3} 2\omega\, \rho_{\bar{q}}(\omega)\, \Theta(\omega)\, n_F((\omega+\mu_q)/T)\; \Theta(\pm P^2) \cdots$$

➔ **Mean-field scalar potential (1PI) for quarks and gluons (U_q, U_g) vs parton scalar density ρ_S:**

$$U_s(\rho_s) = \frac{dV_p(\rho_s)}{d\rho_s} \qquad \rho_S = N_g^{+} + N_q^{+} + N_{\bar{q}}^{+}$$

$$Uq = Us, \quad Ug \sim 2Us$$

Quasiparticle potentials (U_q, U_g) are repulsive !

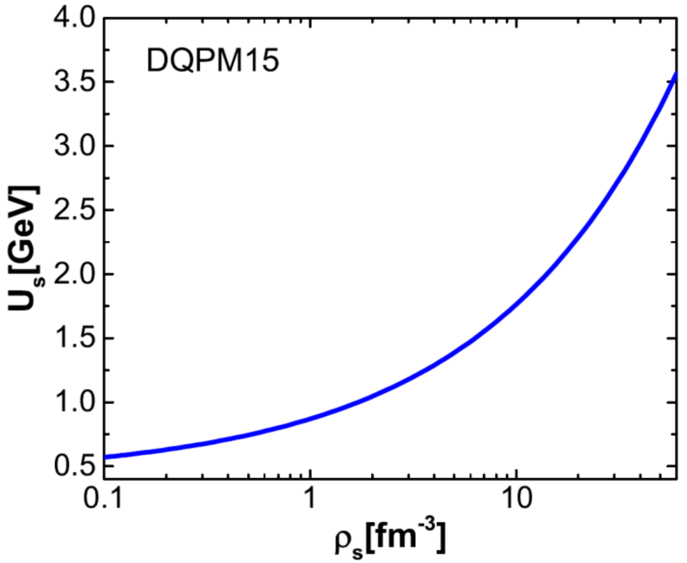

➔ **the force acting on a quasiparticle j:**

$$F \sim M_j/E_j \nabla U_s(x) = M_j/E_j\; dU_s/d\rho_s\; \nabla\rho_s(x)$$

$$j = g, q, \bar{q}$$

➔ **accelerates particles**

Cassing, NPA 791 (2007) 365: NPA 793 (2007)

QGP near equilibrium

DQPM (T, μ_q) :

transport properties at finite (T, μ_q)

Transport coefficients: shear viscosity η at finite (T, μ_q)

Relaxation-Time Approximation (RTA)

(+ cross-check with Kubo formalism):

$$\eta^{\rm RTA}(T,\mu_B) = \frac{1}{15T}\sum_{i=q,\bar{q},g}\int\frac{d^3p}{(2\pi)^3}\frac{\mathbf{p}^4}{E_i^2}\tau_i(\mathbf{p},T,\mu_B)\, d_i(1\pm f_i)f_i$$

$$\tau_i(\mathbf{p},T,\mu_B) = \frac{1}{\Gamma_i(\mathbf{p},T,\mu_B)}$$

Parton interaction rate:

$$\Gamma_i \propto \sum_j d_j\, f_j\, \sigma_{ij}$$

σ_{ij} → leading order diagrams

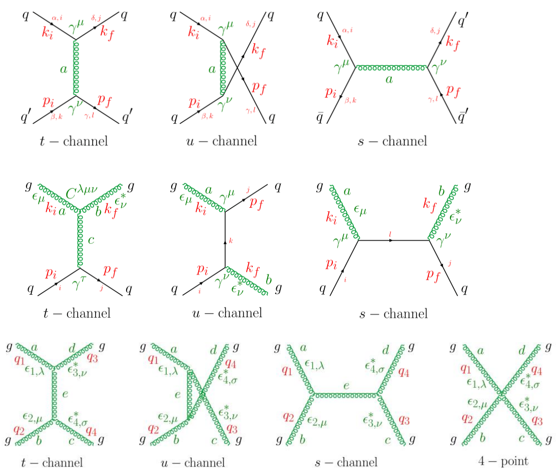

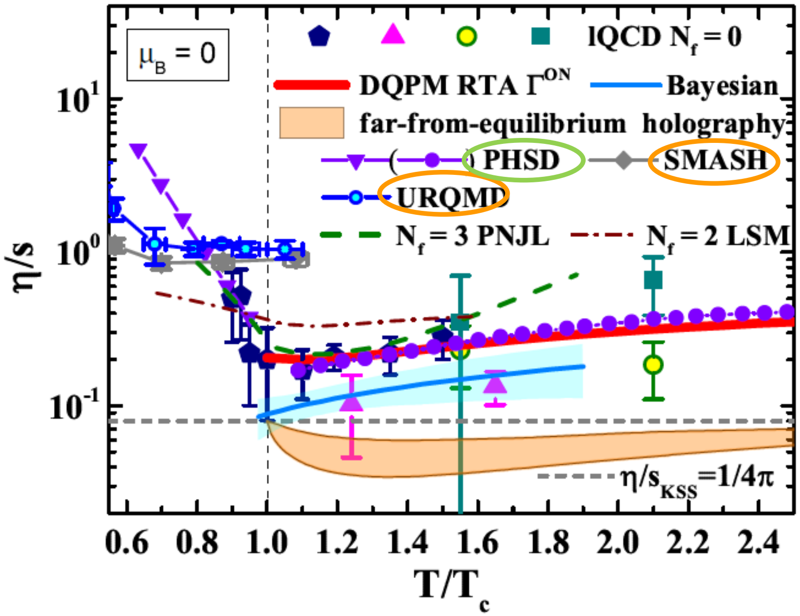

η/s from DQPM = η/s from PHSD in a box

Shear viscosity η/s (T, μ_q)

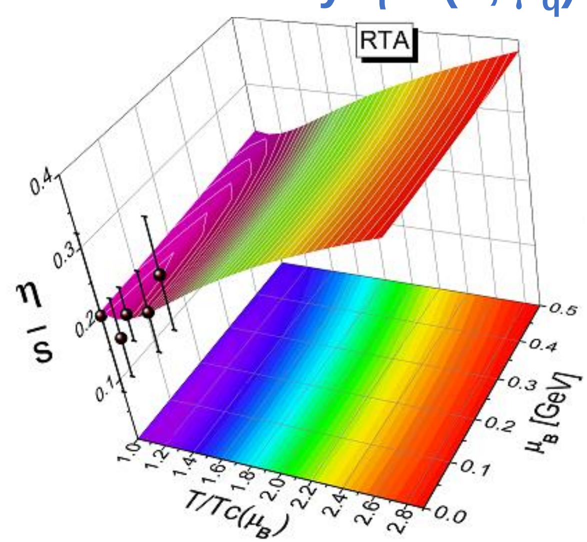

- Good agreement with lQCD
- Light increase of shear viscosity with μ_B

P. Moreau et al., PRC100 (2019) 014911; O. Soloveva et al., PRC110 (2020) 045203

Lattice QCD: N. Astrakhantsev et al, JHEP 1704 (2017) 101

Transport coefficients at finite (T, μ_q)

Baryon diffusion coefficient κ_B/T^2

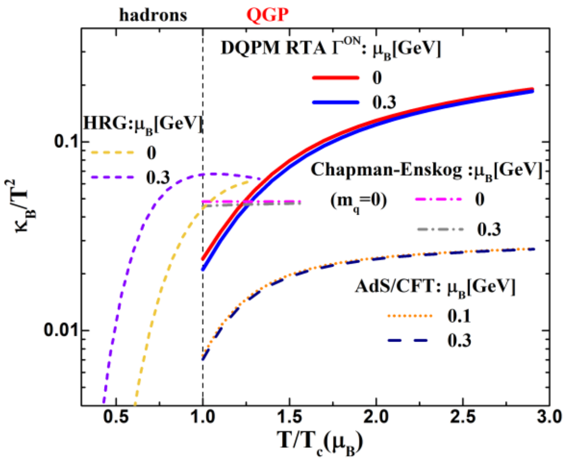

Full diffusion coefficient matrix has been evaluated:

$$\begin{pmatrix} j_B^\mu \\ j_Q^\mu \\ j_S^\mu \end{pmatrix} = \begin{pmatrix} \kappa_{BB} & \kappa_{BQ} & \kappa_{BS} \\ \kappa_{QB} & \kappa_{QQ} & \kappa_{QS} \\ \kappa_{SB} & \kappa_{SQ} & \kappa_{SS} \end{pmatrix} \cdot \begin{pmatrix} \nabla^\mu \alpha_B \\ \nabla^\mu \alpha_Q \\ \nabla^\mu \alpha_S \end{pmatrix}$$

J. A. Fotakis, O. Soloveva, C. Greiner, O. Kaczmarek and E.B.,
PRD 104 (2021) , 034014

O. Soloveva et al., PRC110 (2020) 045203

Electric conductivity σ_e/T

Bulk viscosity ζ/s

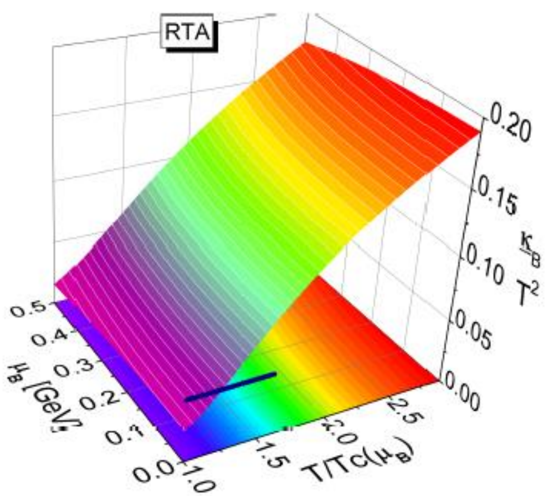

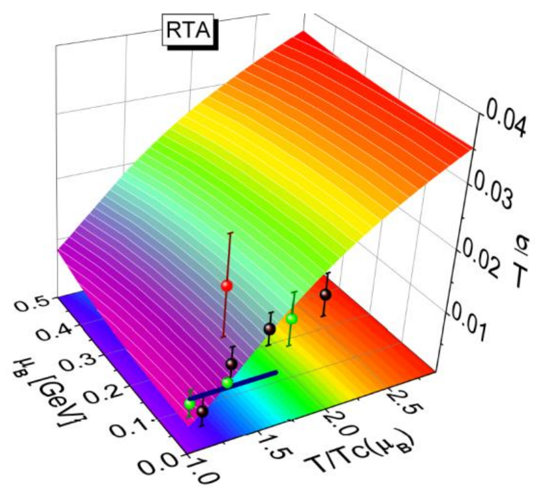

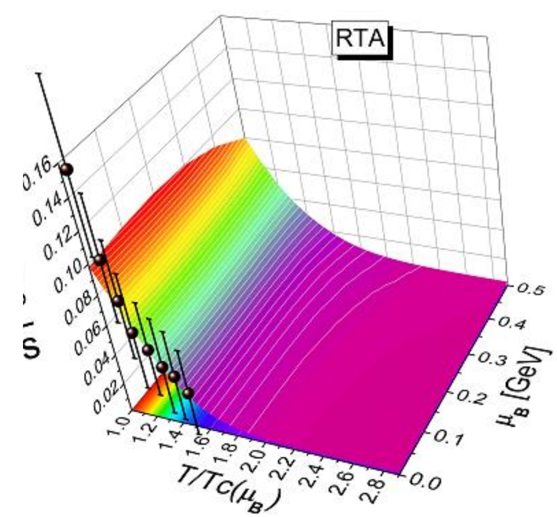

→ **Weak dependence of transport coefficients on μ_B**

Probing of the properties of sQGP with jet partons

Extension of DQPM (T, μ_q)

elastic (2→2) + inelastic (2→3) scattering

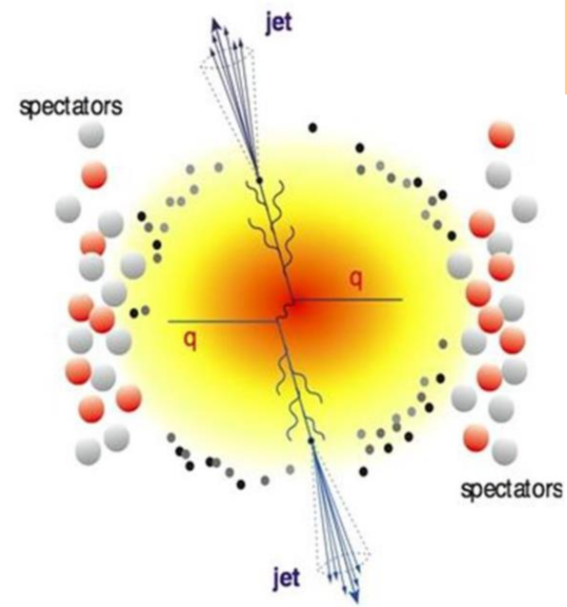

Ilia Grishmanovskii (PhD Thesis)

Partonic inelastic 2→3 interactions

quark + quark

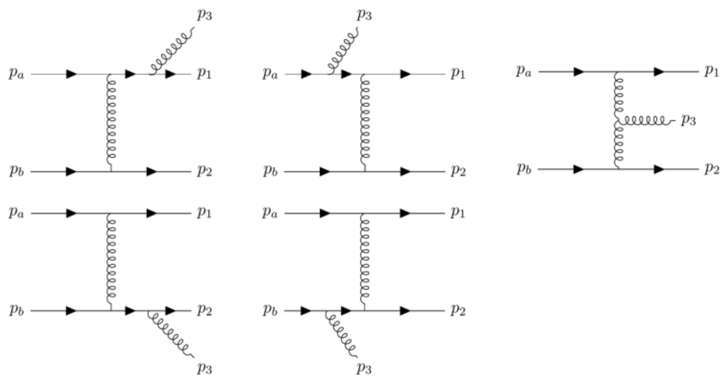

quark + gluon (t-channel)

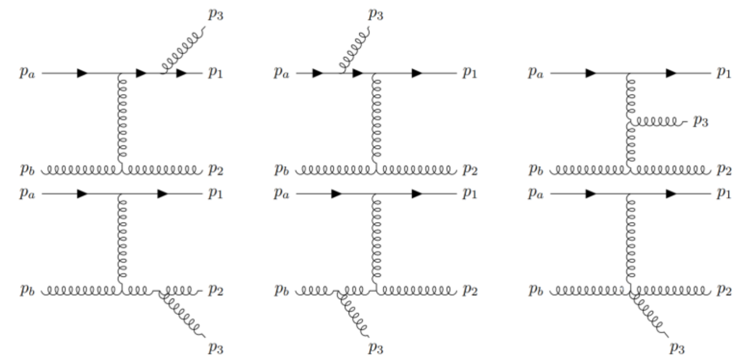

quark + gluon (u-channel)

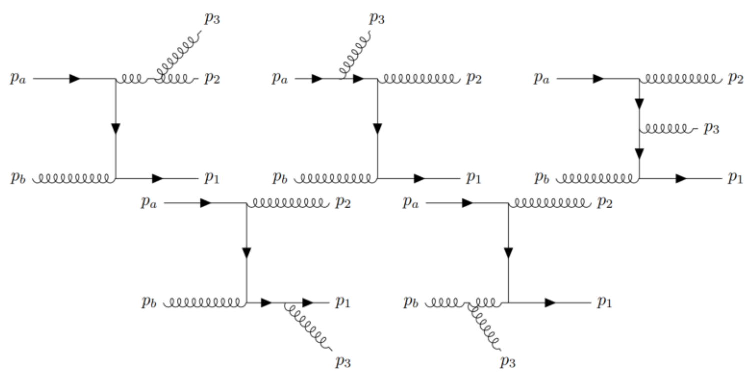

quark + gluon (s-channel)

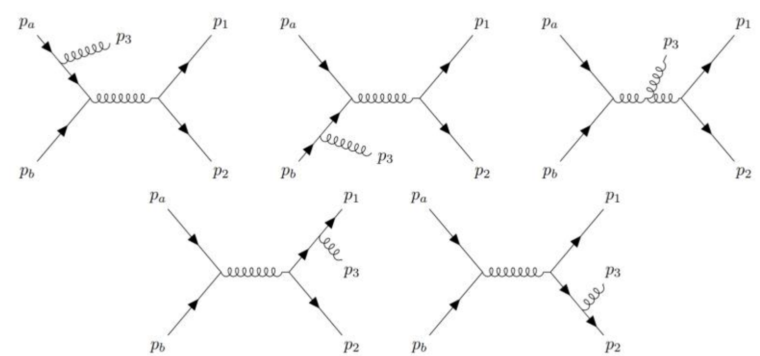

- **No approximations applied**
- **All interference terms included**
- **Emitted gluon is massive in DQPM**

I. Grishmanovskii et al., PRC 109, 024911 (2024)

Partonic cross sections: elastic vs. inelastic

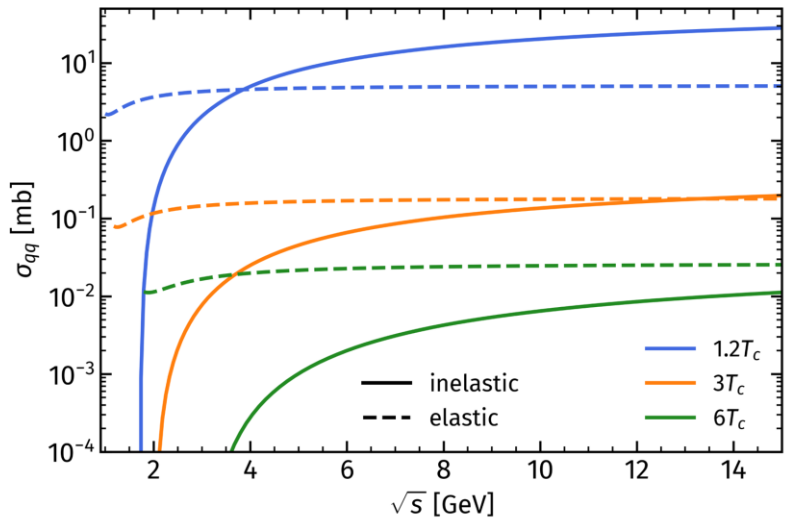

$|\overline{\mathcal{M}}_{2\to2}|^2 \propto \alpha_s^2$

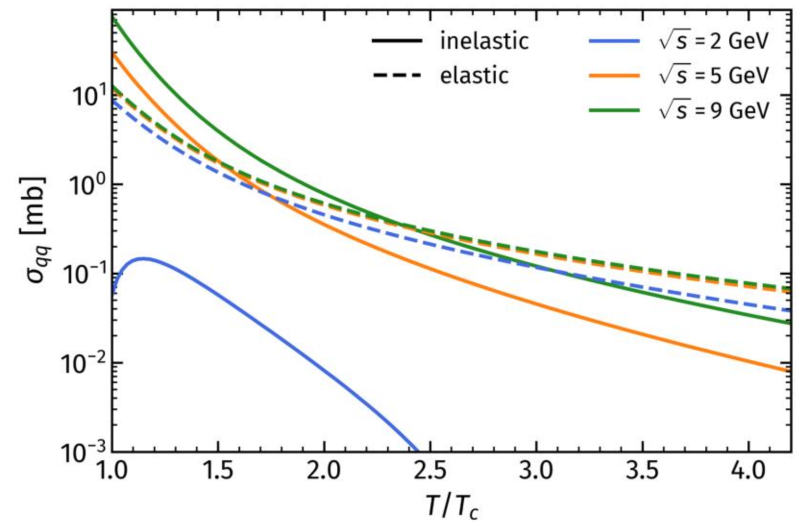

$|\overline{\mathcal{M}}_{2\to3}|^2 \propto \alpha_s^3$

➔ **Elastic cross sections dominate at low energies and high temperatures**

➔ **Inelastic cross sections dominate at high energies and low temperatures**

➔ **Temperature dependence is stronger for the inelastic reactions and is mainly driven by the DQPM strong coupling**

*** In calculations - emitted gluon has a thermal pole mass $m_g^0(T)$**

I. Grishmanovskii et al., PRC 109, 024911 (2024)

Inelastic cross sections: emitted gluon m_g

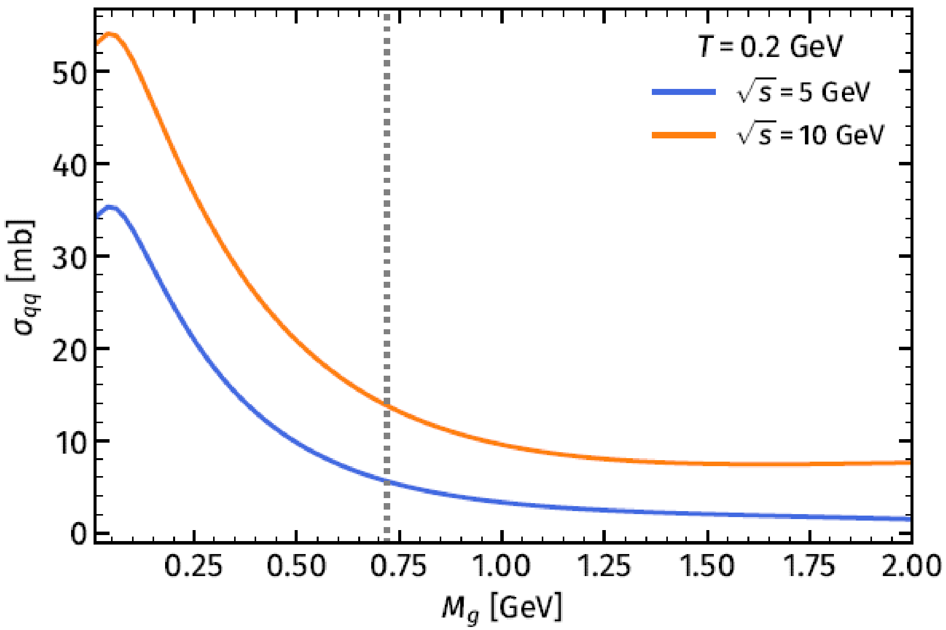

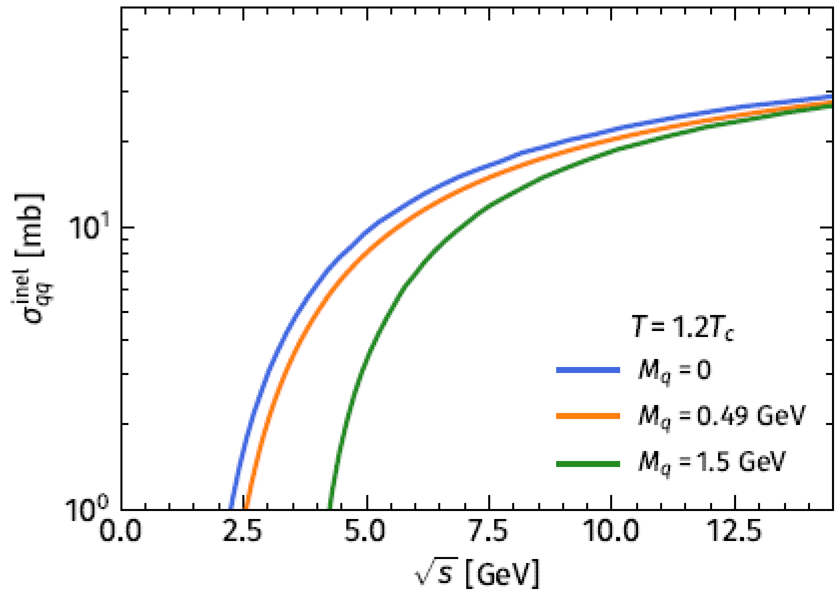

- **Strong dependence of inelastic total cross section on the mass of emitted gluon m_g**
- **Shift of the threshold of inelastic σ_{qq} with increasing m_g**

I. Grishmanovskii et al., PRC 109, 024911 (2024)

Jet transport coefficients from elastic scattering

On-shell:

- **integration over momenta**
- **masses = pole masses**

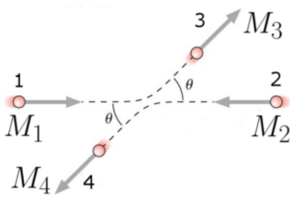

$$E^2 = m^2 + p^2$$

$$\langle \mathcal{O} \rangle^{\text{on}} = \frac{1}{2E_i} \sum_{j=q,\bar{q},g} d_j f_j \int \frac{d^3 p_j}{(2\pi)^3 2E_j} \times \int \frac{d^3 p_1}{(2\pi)^3 2E_1} \int \frac{d^3 p_2}{(2\pi)^3 2E_2} \times (1 \pm f_1)(1 \pm f_2)\mathcal{O}|\overline{\mathcal{M}}|^2 (2\pi)^4 \delta^{(4)}(p_i + p_j - p_1 - p_2)$$

Off-shell:

- **integration over momenta**
- **+ two additional integrations over medium parton energies**

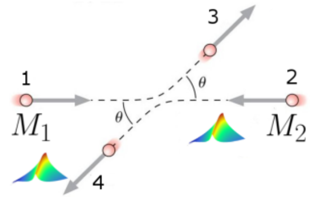

$$\frac{1}{2E} \to \int \frac{d\omega}{(2\pi)} \rho(\omega, \mathbf{p}) \theta(\omega)$$

$$\langle \mathcal{O} \rangle^{\text{off}} = \frac{1}{2E_i} \sum_{j=q,\bar{q},g} d_j f_j \int \frac{d^4 p_j}{(2\pi)^4} \rho(\omega_j, \mathbf{p}_j)\theta(\omega_j) \times \int \frac{d^3 p_1}{(2\pi)^3 2E_1} \int \frac{d^4 p_2}{(2\pi)^4} \rho(\omega_2, \mathbf{p}_2)\theta(\omega_2) \times (1 \pm f_1)(1 \pm f_2)\mathcal{O}|\overline{\mathcal{M}}|^2 (2\pi)^4 \delta^{(4)}(p_i + p_j - p_1 - p_2)$$

$$\langle \mathcal{O} \rangle_u = \sum_q \langle \mathcal{O} \rangle_{uq} + \sum_{\bar{q}} \langle \mathcal{O} \rangle_{u\bar{q}} + \langle \mathcal{O} \rangle_{ug} = \langle \mathcal{O} \rangle_{uu\to uu} + \langle \mathcal{O} \rangle_{ud\to ud} + \langle \mathcal{O} \rangle_{us\to us} + \langle \mathcal{O} \rangle_{u\bar{u}\to u\bar{u}} + \langle \mathcal{O} \rangle_{u\bar{d}\to u\bar{d}} + \langle \mathcal{O} \rangle_{u\bar{s}\to u\bar{s}} + \langle \mathcal{O} \rangle_{ug\to ug}$$

- **Scattering rate Γ :** $\mathcal{O} = 1$
- **Transverse momentum transfer squared per unit length $\hat{q}$:** $\mathcal{O} = |\vec{p_T} - \vec{p_T}'|^2 \to \langle O \rangle = \hat{q}$
- **Energy loss per unit length dE/dx:** $\mathcal{O} = (E - E') \to \langle O \rangle = dE/dx$
- **Drag coefficient A:** $\mathcal{O} = p_L - p'_L$

Partonic interaction rates in equilibrated sQGP

Interaction rate

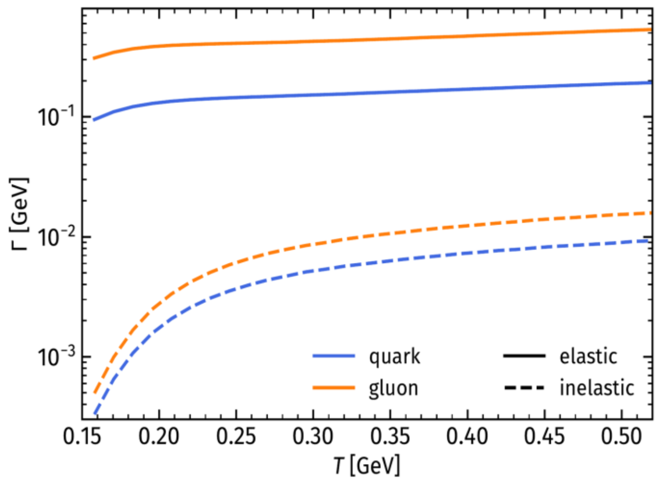

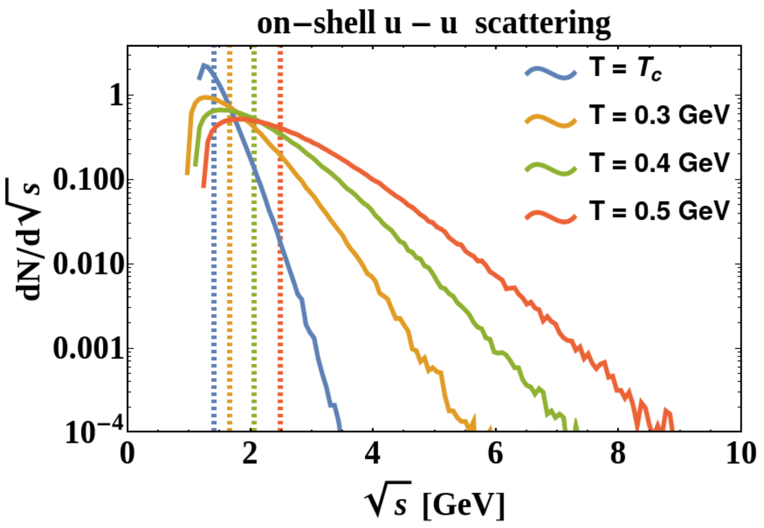

In thermalized QGP low energies are favored where the elastic scatterings dominate

Relaxation time (τ ~ 1/Γ)

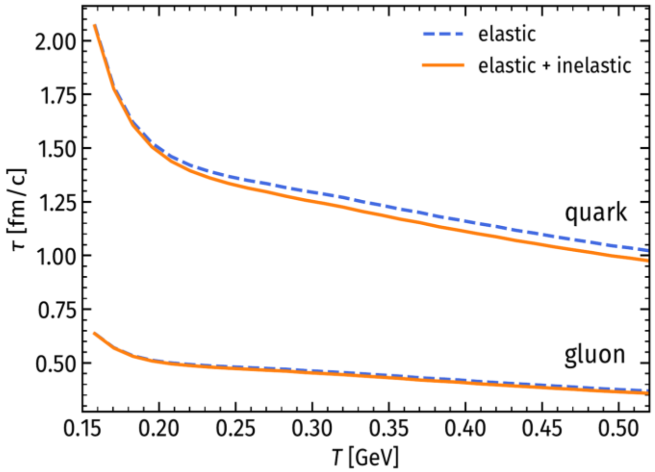

- ➔ **The partonic interaction rates and relaxation time are primarily governed by elastic scattering**
- ➔ **Inelastic processes – with massive gluon emission – are suppressed in the thermalized QCD medium**

I. Grishmanovskii et al., PRC 109, 024911 (2024)

$\hat{q}$ from elastic scattering

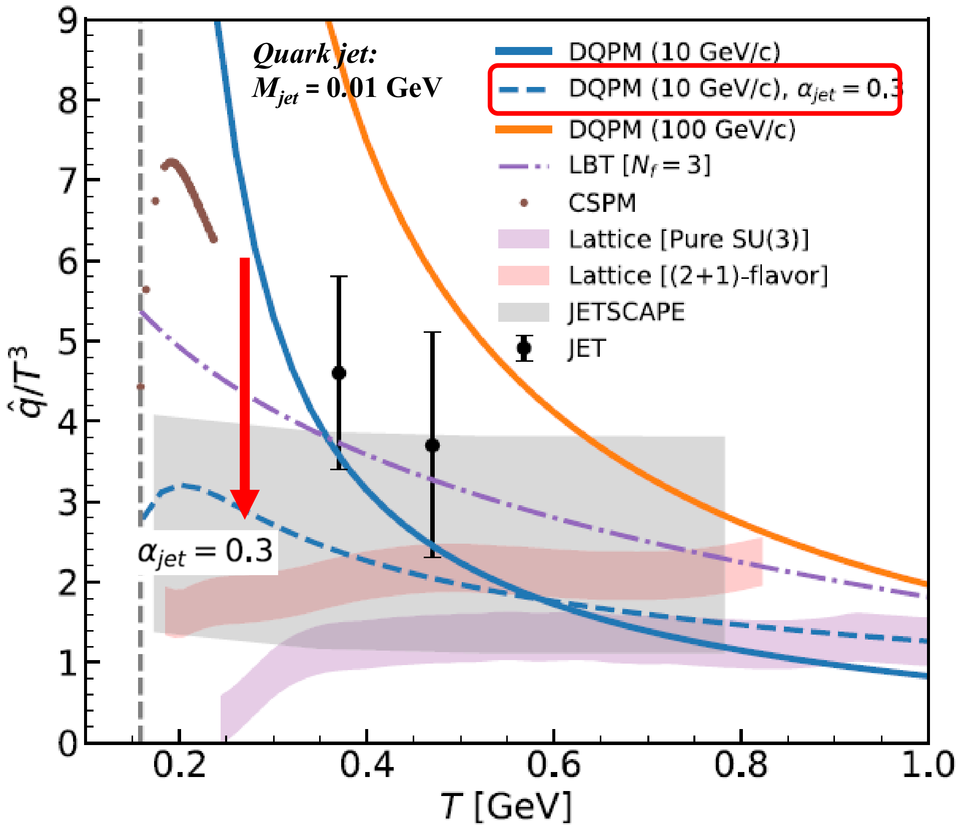

➔ Agreement with the other models at low jet energy

➔ Rapid rise with decreasing medium temperature due to strong increase of g(T)

I. Grishmanovskii et al., Phys. Rev. C 106, 014903 (2022)

$\hat{q}$ and dE/dx from elastic scattering

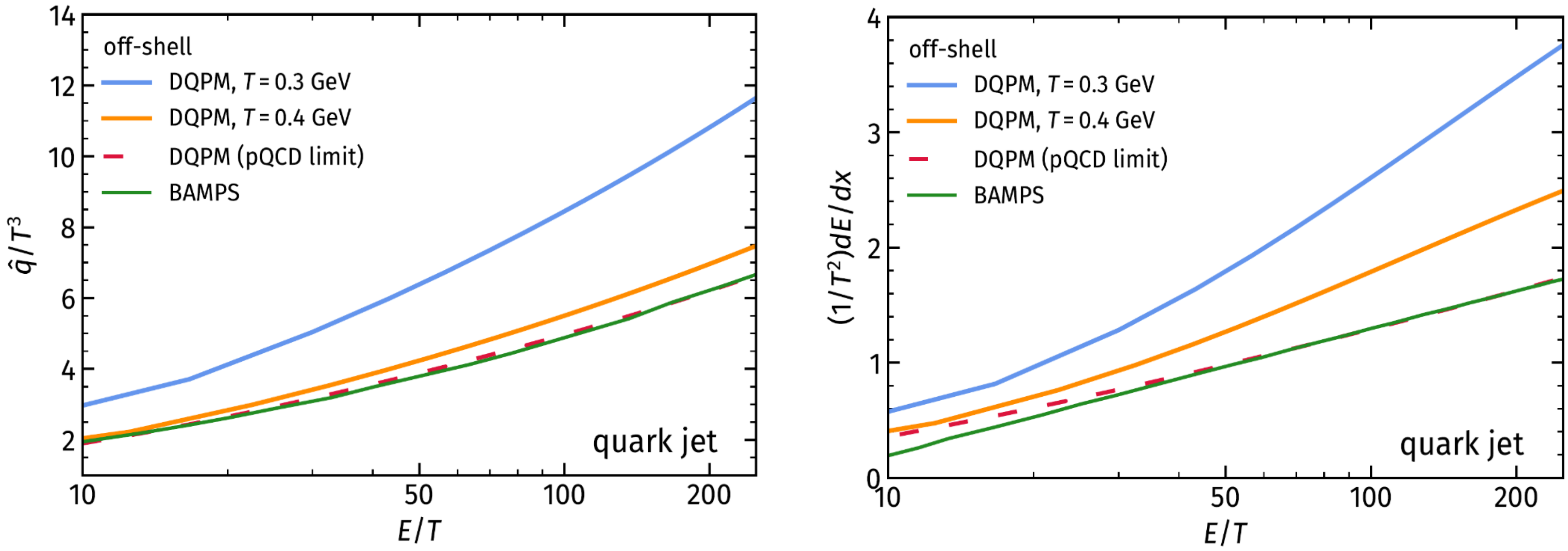

➔ **Logarithmic growth of q-hat and energy loss dE/dx with jet energy E**

➔ **DQPM predicts stronger suppression than pQCD**

➔ **Aligning with pQCD-based calculations in the pQCD-limit**

I. Grishmanovskii et al., PRC 106, 014903 (2022)

$\hat{q}$ from elastic (2→2) vs. inelastic (2→3) scattering

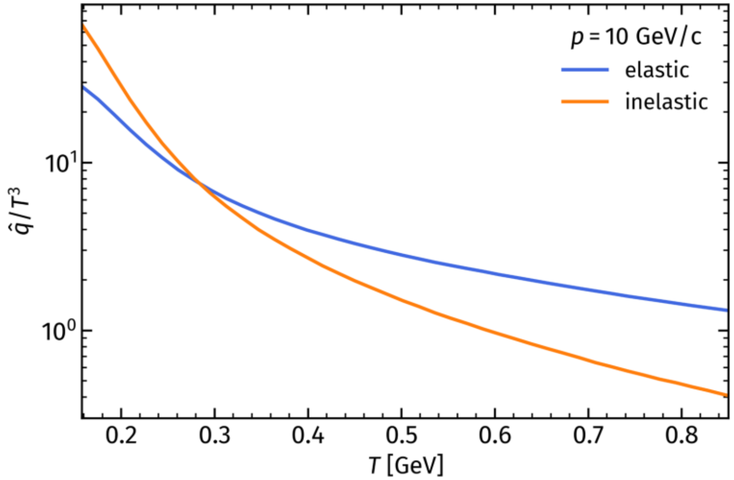

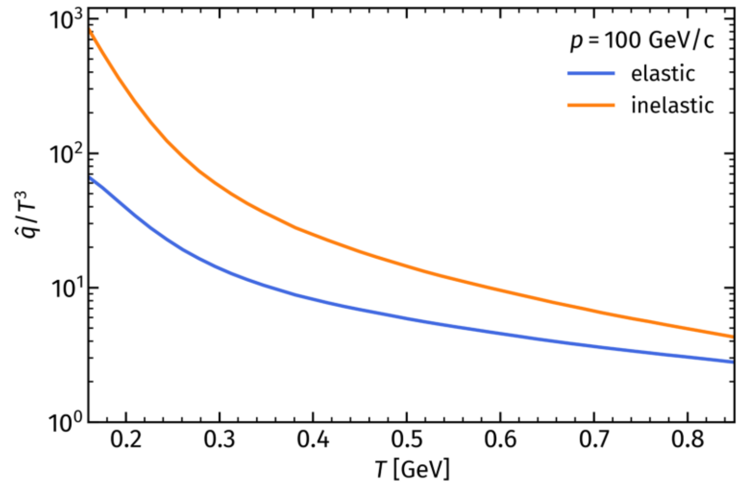

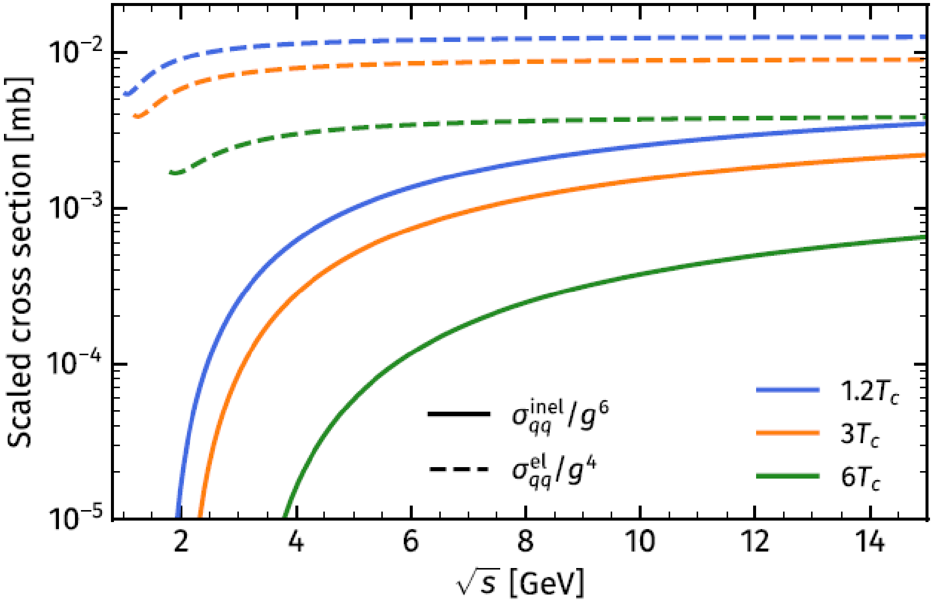

➔ **Strong dependence of elastic (~g^4) and inelastic (~g^6) cross sections on strong coupling constant**

➔ **Temperature and momentum dependence is stronger for inelastic reactions**

➔ **Stronger energy loss at large energies and small temperatures**
→ **questionable suppression of jets in heavy-ion collisions**

I. Grishmanovskii et al., PRC 110, 014908 (2024)

Different scenarios for strong couplings

- Jet is not a part of the QGP medium → strong coupling is not thermal
  → consider different strong couplings
  in *thermal* (green), *jet* (blue), and *radiative* (red) vertices

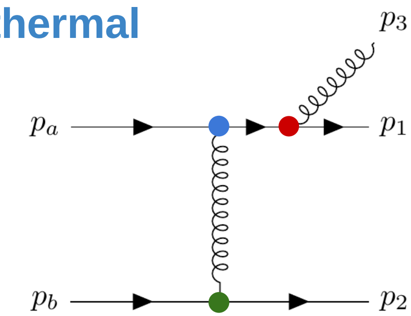

	Vertex		
Model	• medium parton	• jet parton	• emitted gluon
Scenario 0	$g^{\mathrm{DQPM}}(T)$		
Scenario I	$g = \sqrt{4\pi \times 0.3}$		
Scenario II	$g^{\mathrm{DQPM}}(T)$	$g(Q^2)$	$g(k_t^2)$
Scenario III	$g^{\mathrm{DQPM}}(T)$	$g(E)$	$g(E)$
Scenario IV	$g^{\mathrm{DQPM}}(T)$	$g(ET)$	$g(Q^2)$

Scenario 0 → "default" DQPM (thermal coupling)

Scenario I → constant strong coupling

Scenario II: **Zakharov model**; Scenario III: **QLBT model**; Scenario IV: **DREENA framework** →

$$g^2(t) = \frac{48\pi^2}{(11N_c - 2N_f)} \frac{1}{\ln\left(\frac{t}{\Lambda^2}\right)}$$

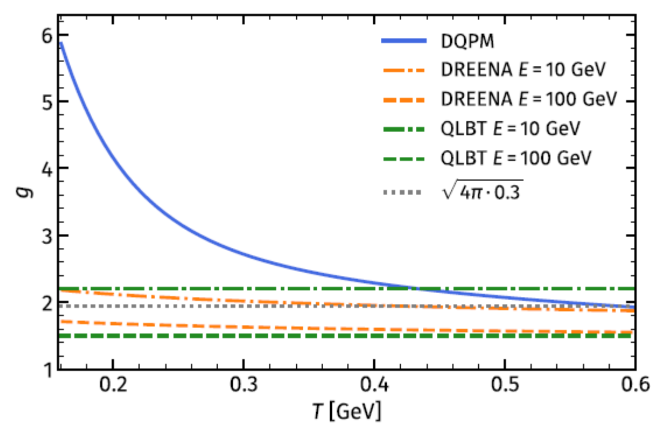

[II] B. G. Zakharov, JETP Lett. 112, 681 (2020).
[III] F.-L. Liu et al., Eur. Phys. J. C 82, 350 (2022).
[IV] D. Zigic et al, Front. Phys. 10, 957019 (2022).

I. Grishmanovskii et al., PRC 110, 014908 (2024)

$\hat{q}$ from elastic + inelastic scattering

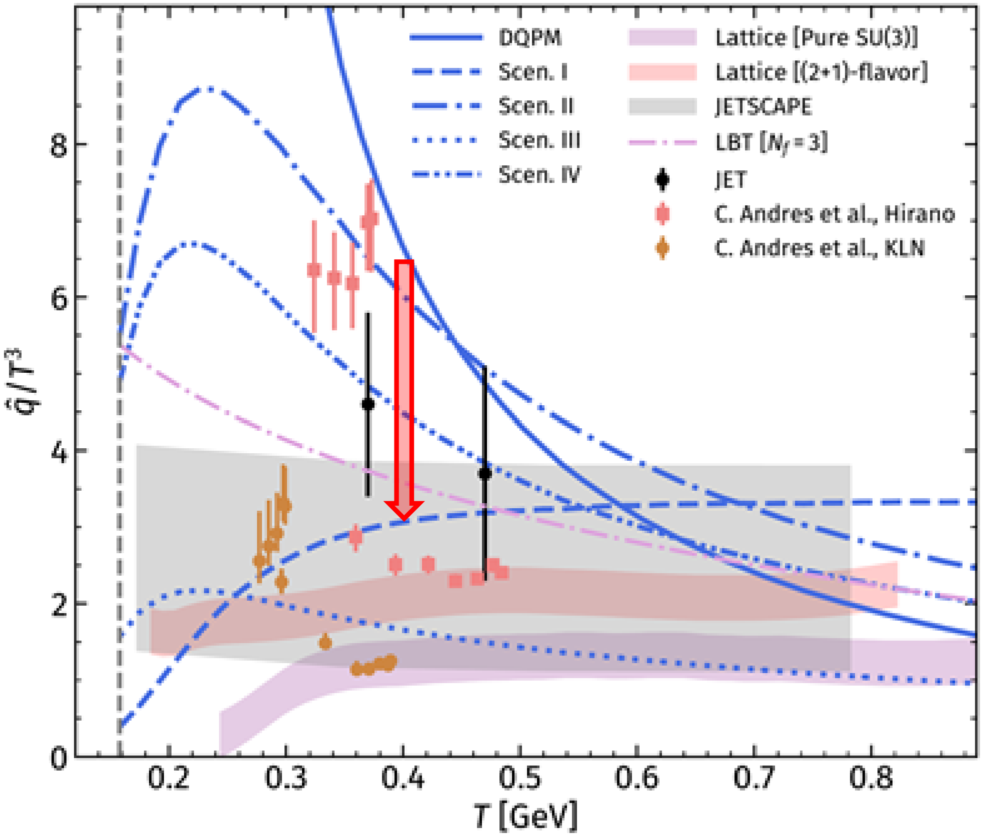

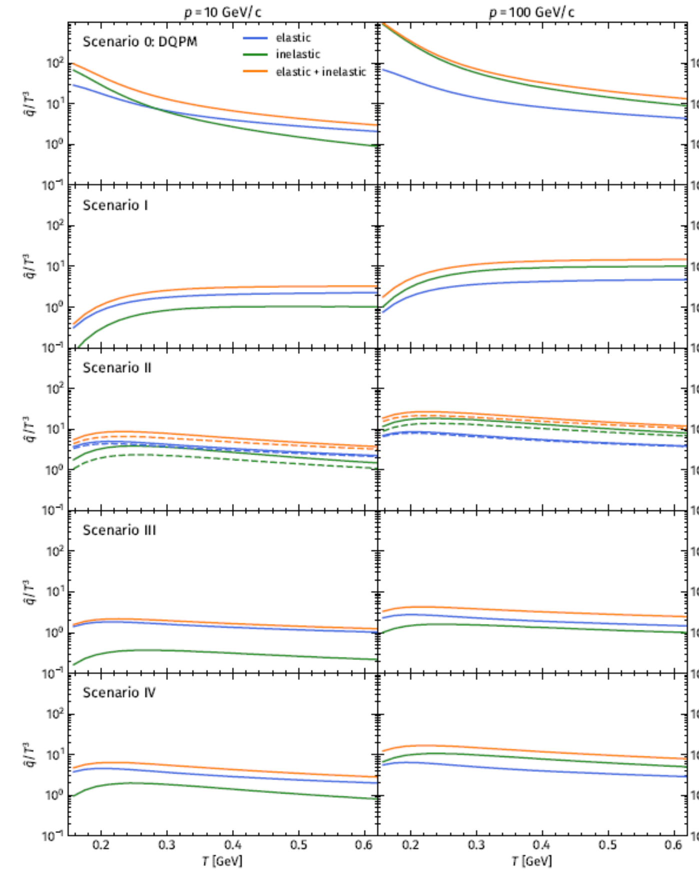

➔ **High sensitivity to the choice of the strong coupling (“scenario”)**

➔ **The “default” DQPM with the thermal couplings produces the highest values of the transport coefficients**

I. Grishmanovskii et al., PRC 110, 014908 (2024)

dE/dx from elastic + inelastic scattering

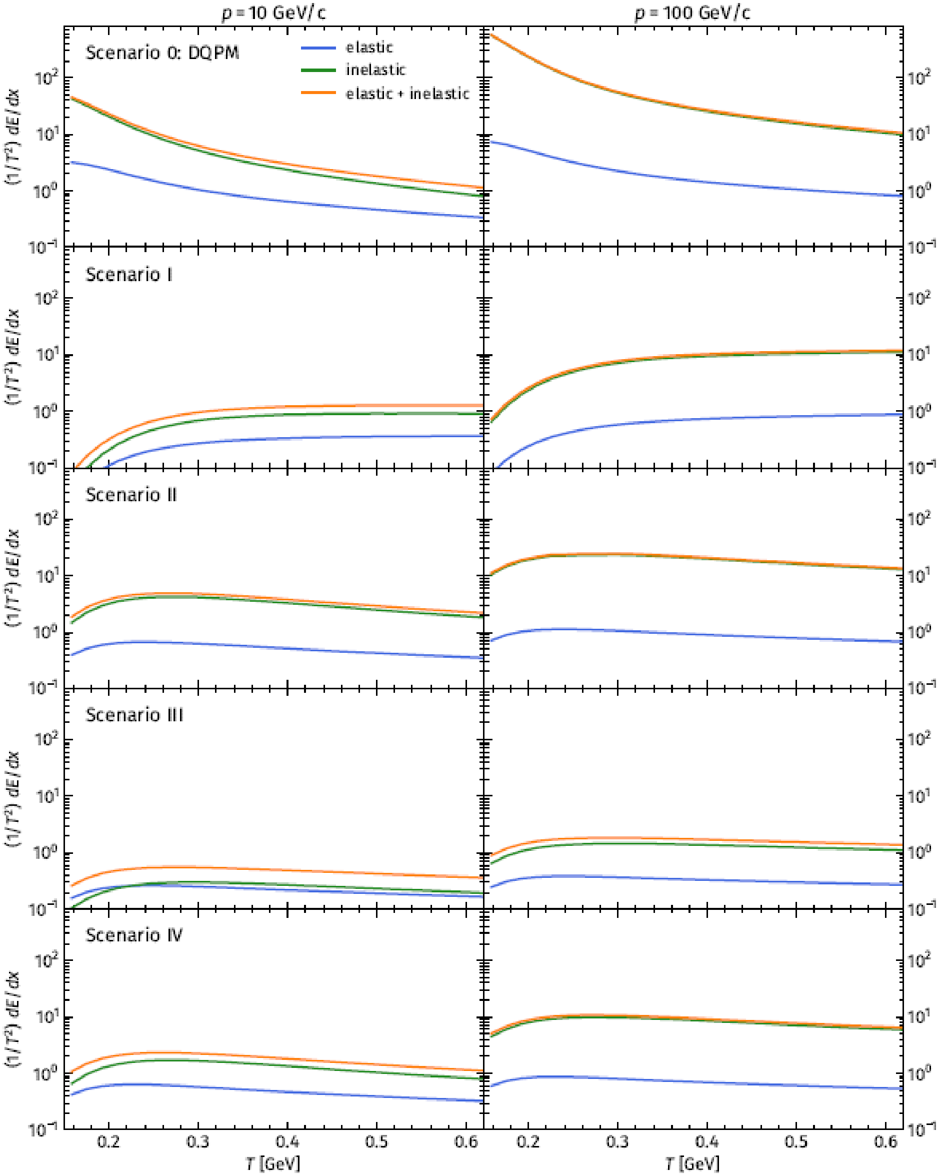

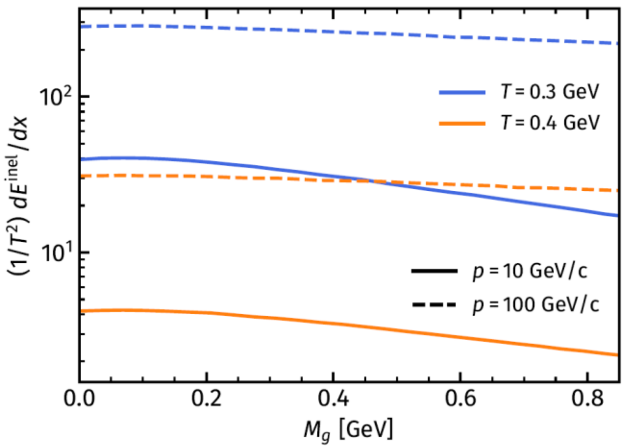

→ **High sensitivity to the choice of the strong coupling ("scenario")**

→ **The "default" DQPM with the thermal couplings produces the highest energy loss**

→ **Energy loss is decreasing with increasing m_g**

I. Grishmanovskii et al., PRC 110, 014908 (2024)

Relation between η/s and $\hat{q}$

In the weak coupling limit:

B. Müller, PRD 104, L071501 (2021)

$$\eta/s \approx 1.25\,\frac{T^3}{\hat{q}}$$

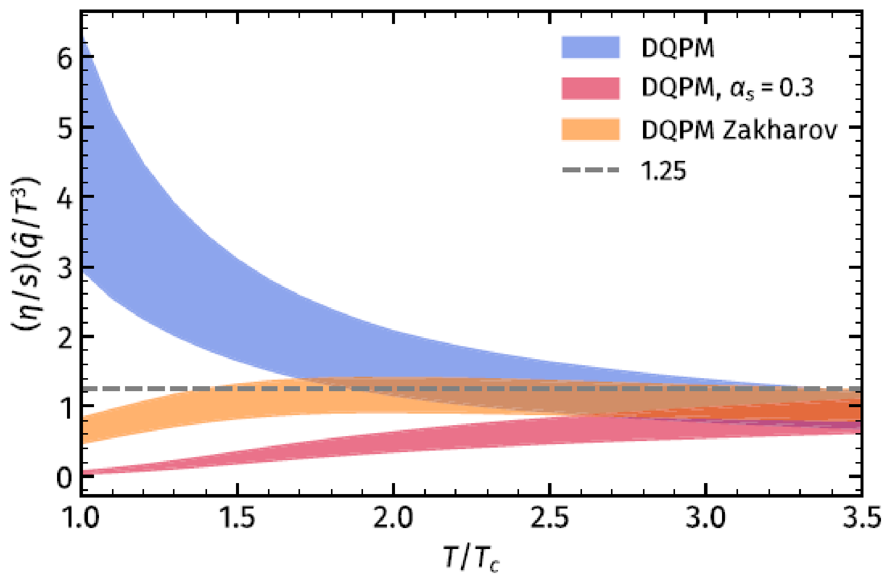

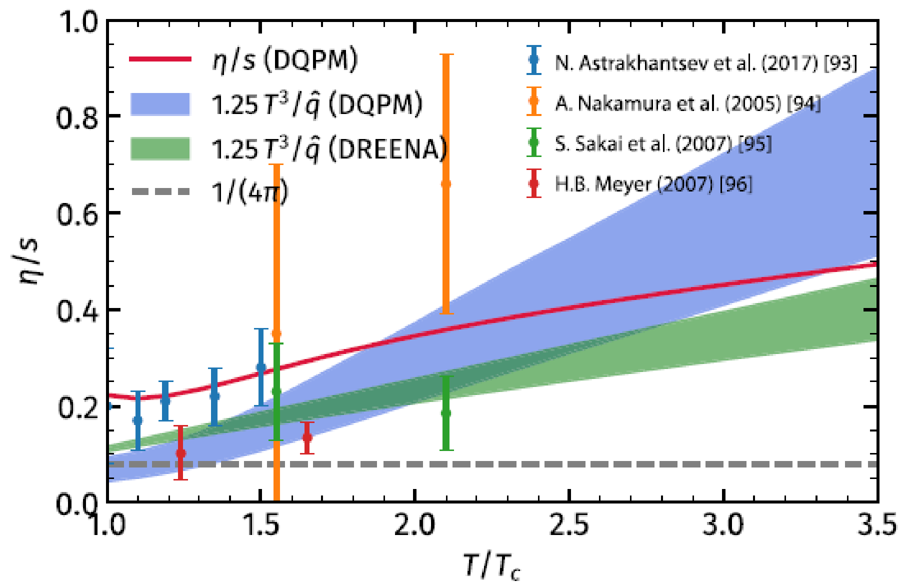

➔ **Sensitive to the choice of the strong coupling**

➔ **Valid in the weak coupling regime (at high temperatures)**

➔ **Violated in the strong coupling regime (at low temperatures)**

I. Grishmanovskii et al., PRC 110, 014908 (2024)

QGP:
in-equilibrium → off-equilibrium

Microscopic transport theory!

DQPM → PHSD

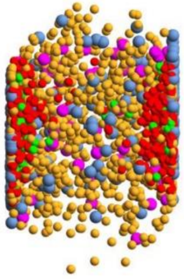

* QGP: only elastic partonic interactions
are implemented in the PHSD up to now

Dynamical modeling of heavy-ion collisions - PHSD

Parton-Hadron-String Dynamics (PHSD) is a non-equilibrium microscopic transport approach for the description of dynamics of strongly-interacting hadronic and partonic matter created in heavy-ion collisions

Dynamics: based on the solution of generalized off-shell transport equations derived from Kadanoff-Baym many-body theory (beyond semi-classical BUU)

Initial state: Au+Au | Quark-Gluon Plasma: lQCD EoS non-perturbative QCD - quasiaprticles | Dynamical Hadronization | Hadronic interactions ➔final hadrons + leptons

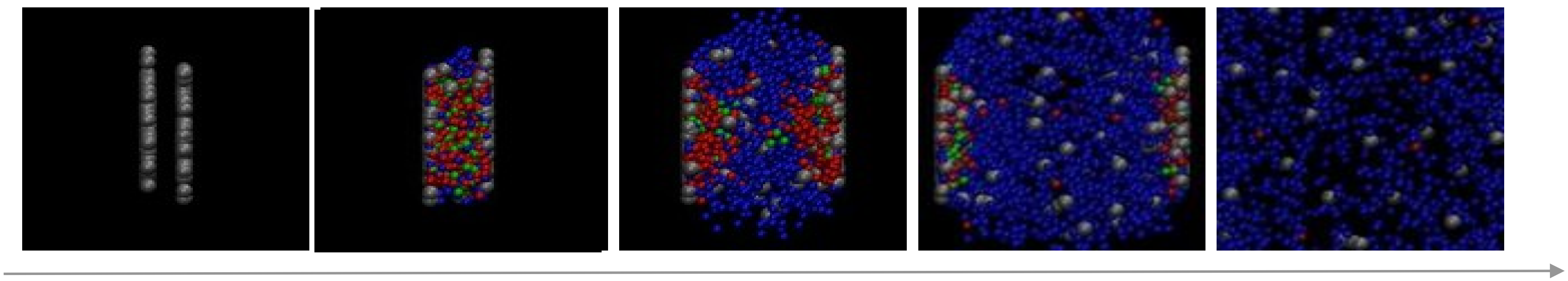

time

- ➔ PHSD provides a good description of 'bulk' hadronic and electromagnetic observables from SIS to LHC energies
- ➔ PHSD/PHQMD is a tool to study dynamics of HICs; under constant development to account for the complexity of HICs on a microscopic basis

PHSD/PHQMD are open source codes, available for all experimental collaborations (used by GSI/FAIR collaborations, linked to the exp. software) and upon registration for other users

PHSD: W. Cassing, E. Bratkovskaya, PRC 78 (2008) 034919; NPA831 (2009) 215; P. Moreau et al., PRC100 (2019) 014911

Traces of the QGP at finite μ_q in observables

Input: ε^{PHSD} and n_B^{PHSD} → lQCD → **Output:** T, μ_B

$$\frac{n_B}{T^3} \approx \chi_2^B(T)\left(\frac{\mu_B}{T}\right) + \ldots$$

$$\Delta\epsilon/T^4 \approx \frac{1}{2}\left(T\frac{\partial\chi_2^B(T)}{\partial T} + 3\chi_2^B(T)\right)\left(\frac{\mu_B}{T}\right)^2 + \ldots$$

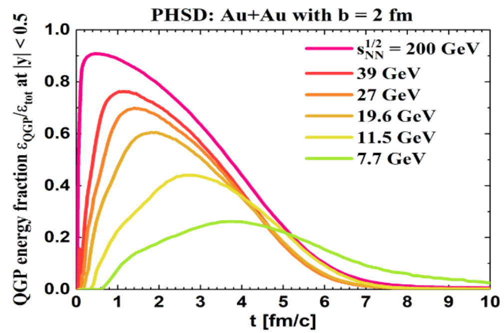

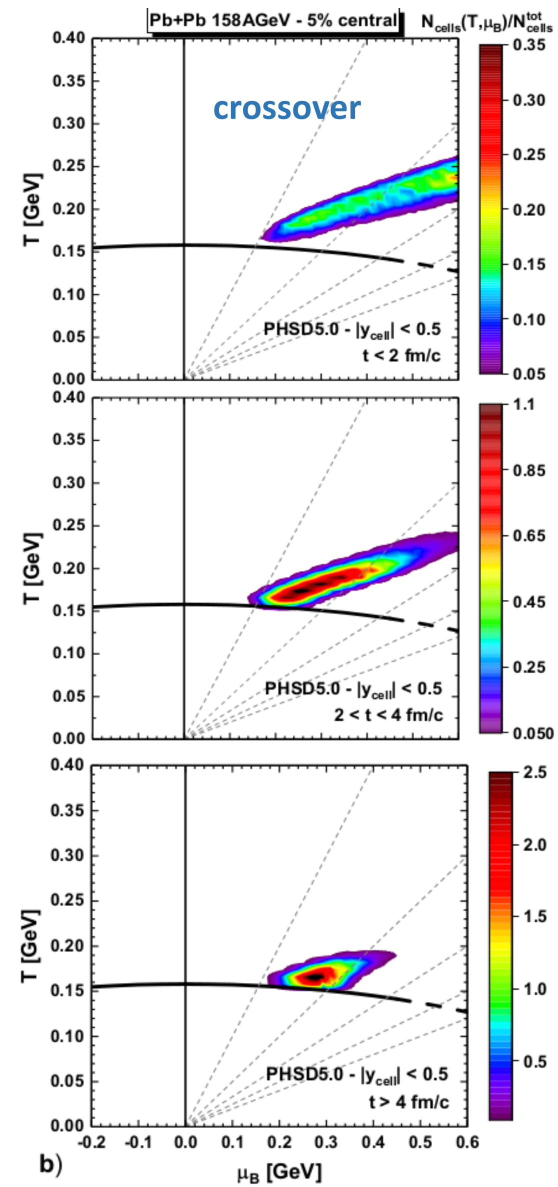

Flow: v_1 Au+Au, 27GeV, 10-40%

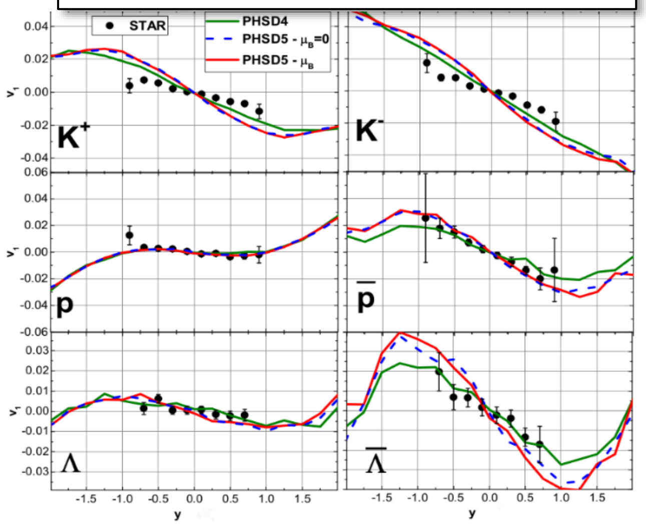

v_2: 200GeV, 10-20% central

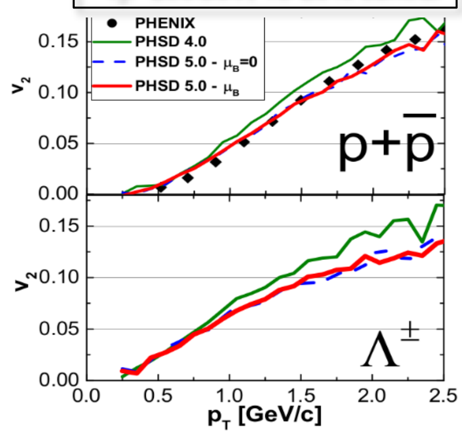

- **Weak μ_B –dependence of v_1, v_2** due to a small fraction of QGP at low energies or low μ_B (at high energies)
- **Strong flavor dependence– strange antibaryons are more sensitive to μ_B**

P. Moreau et al., PRC 100 (2019) , 014911

O. Soloveva et al., Particles 3 (2020) 178

Summary

- DQPM provides a **self-consistent approach** to study **partonic interactions** and **transport properties** of the sQGP
- **Inelastic** interactions are **suppressed** in a thermalized QGP medium, but are **crucial** in the context of **jet attenuation**
- **Jet energy loss** of hard jet partons is **larger** within the DQPM compared to the pQCD-based calculations
- **Transport coefficients** are highly **sensitive** to the choice of the **strong coupling**

Outlook:

- Implement inelastic $2 \rightarrow 3$ cross sections into full transport simulation (PHSD)
- Study the full jet evolution within transport simulations
- Implement the LPM effect